Directing Nuclear Spin Flips in InAs Quantum Dots Using Detuned Optical Pulse Trains

S. G. Carter,[1] A. Shabaev,[2] Sophia E. Economou,[1] T. A. Kennedy,[1] A. S. Bracker,[1] and T. L. Reinecke[1]

[1]*Naval Research Laboratory, Washington, D.C. 20375-5322, USA*

[2]*School of Computational Sciences, George Mason University, Fairfax, Virginia 22030, USA*

(Received 11 December 2008; published 24 April 2009)

We find that detuning an optical pulse train from electronic transitions in quantum dots controls the direction of nuclear spin flips. The optical pulse train generates electron spins that precess about an applied magnetic field, with a spin component parallel to the field only for detuned pulses. This component leads to asymmetry in the nuclear spin flips, providing a way to stabilize and control the nuclear spin polarization. This effect is observed using two-color, time-resolved Faraday rotation and ellipticity.

DOI: 10.1103/PhysRevLett.102.167403 PACS numbers: 78.67.Hc, 72.25.Fe, 78.47.jc

Spins in semiconductor quantum dots (QDs) are promising quantum bits, with spin coherence times of a few microseconds [1,2], controlled interactions with other QDs [3], and fast optical initialization and control [4–7]. A point of considerable current interest for QDs as qubits is the hyperfine interaction with the many (10^4–10^5) nuclei in the dot [8–23]. The nuclear spin configuration is typically random and varying in time, changing the electron-spin (*e*-spin) splitting by creating an effective magnetic field for the electron (Overhauser shift). This leads to an apparent *e*-spin dephasing time T_2^* of a few nanoseconds and a varying spin splitting. This can be overcome by pumping nuclear spins into a narrow distribution of states. Indirect control of the nuclei through *e*-spin manipulation has been explored both electrically [21] and optically [11–13,17–20], with nuclear polarizations reaching ~40% in recent experiments on single InGaAs dots [12,18,20].

In Ref. [19], periodic excitation by an optical pulse train is used in an ensemble of QDs with inhomogeneous *e*-spin precession frequencies. Those spins synchronized to a multiple of the laser repetition rate are not affected by the laser pulses, and the electron-nuclear dynamics are uninterrupted. The nuclei in QDs with nonsynchronized *e* spins are indirectly affected by the optical excitation, and have a higher probability of spin flip. With no *e*-spin polarization along the magnetic field direction, the nuclei flip up or down with equal probability. Thus, the nuclear polarization takes a random walk, as does the Overhauser shifted *e*-spin precession frequency, until reaching a synchronized precession frequency with a lower nuclear spin-flip rate.

In this Letter, we show that a detuned optical pump train plays a useful role in the nuclear spin dynamics by inducing a steady-state spin component along the magnetic field direction [S_x in Fig. 1(b)] for nonsynchronized *e* spins. This is because the pulse hits the *e* spins when they have a nonzero S_y component and rotates them around the *z* axis. Through hyperfine coupling, the S_x *e*-spin component introduces an asymmetry to the two directions of nuclear spin-flip rates, allowing for accumulation of nuclear spin polarization. The sign of the detuning determines whether the spins are pushed away from or toward a synchronized precession frequency. As a result, a systematic element is added to the electron-nuclear spin dynamics of Ref. [19]. We present experimental optical signatures of the directional nuclear spin dynamics in an ensemble of QDs using two-color, time-resolved Faraday rotation and ellipticity measurements. These results open the way for precise control of the nuclear polarization and a better understanding of the role of the nuclei in *e*-spin manipulation.

The experiments are performed on a sample consisting of 20 layers of InAs QDs, grown by molecular beam epitaxy through Stransky-Krastanov self-assembly. The QDs were grown using the In-flush technique [24], giving a truncated pyramid structure of height 2.5 nm and lateral dimensions varying from 10 to 20 nm. A significant fraction (roughly 50%) of the QDs are singly charged with electrons. The photoluminescence of the QD sample at ~5 K is given in Fig. 1(a), showing a broad spectrum due to inhomogeneity, with a FWHM of ~50 meV.

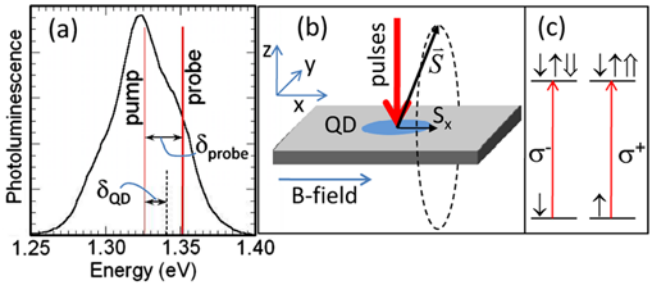

FIG. 1 (color online). (a) Photoluminescence of the quantum dots. The solid vertical lines represent the pump and probe, and the dashed vertical line represents an arbitrary QD energy. (b) Experimental geometry showing spin precession. (c) Electron-trion level diagram, showing the two electron and trion spin states and the allowed transitions. Single (double) arrows are electron (hole) spins.

Electron-spin dynamics are measured with two-color time-resolved Faraday rotation (TRFR) and ellipticity (TRFE). A circularly polarized pump laser spectrally fixed at the center of the photoluminescence [see Fig. 1(a)] excites a distribution of QDs with varying detunings δ_{QD} from the pump. A delayed, vertically polarized probe laser with variable detuning from the pump δ_{probe} measures the pump-induced polarization rotation or ellipticity for a distribution of QDs near the probe photon energy. Rotation (ellipticity) is due to the induced phase (amplitude) difference between the σ^+ and σ^- components of the probe.

Both lasers are wavelength tunable mode-locked Titanium:sapphire lasers operating at a repetition rate of 81 MHz. The pump laser is set to a photon energy of 1.326 meV with a bandwidth of 0.6 meV, corresponding to a Fourier-limited pulse width of 3 ps, and the probe laser has a bandwidth of 1.3 meV, corresponding to 1.4 ps. The average probe intensity is typically $\sim 20\ \mathrm{W/cm^2}$.

Figure 2(a) displays TRFR and the TRFE for $\delta_{\mathrm{probe}} = 0$ at an average pump intensity of $\sim 60\ \mathrm{W/cm^2}$. The magnetic field is 3 T, perpendicular to the optical axis [see Fig. 1(b)]. The oscillating signal is the z component of the

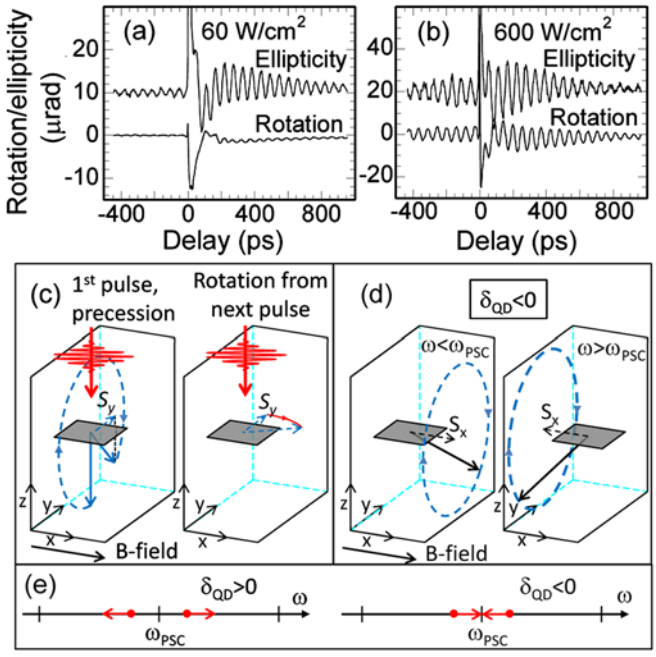

FIG. 2 (color online). (a,b) Time-resolved Faraday rotation and ellipticity for zero pump-probe detuning, taken at an average pump intensity of (a) $\sim 60\ \mathrm{W/cm^2}$ and (b) $\sim 600\ \mathrm{W/cm^2}$ for $B = 3$ T. The ellipticity curves are offset for clarity. (c) Illustration of how detuned pulses generate S_x for nonsynchronized QDs. (d) Illustration of the steady-state e-spin polarization for negatively detuned QDs precessing just slower or faster than the closest PSC. Solid arrows show the e-spin vector just before a pulse. (e) Illustration of changes in ω due to nuclear spin flips for QDs nearby a PSC.

e spin, measured by the probe as it precesses about the external magnetic field. The decay time of 450 ps is due to inhomogeneity in g_e, confirmed by our magnetic field studies. The TRFR shows similar behavior to the TRFE, but with a weaker signal. TRFR and TRFE measure the real and imaginary part of the susceptibility, i.e., dispersion and absorption, respectively. These are generally known to be odd and even functions of the detuning from the transition [25]. Thus, at $\delta_{\mathrm{probe}} = 0$, the TRFR should be near zero, and the TRFE should be at a maximum.

The e-spin polarization is generated by optical pumping through the trion state. As shown in Fig. 1(c), where the spin states are shown in the z basis (along the optical axis), σ^+ light depletes the $|\uparrow\rangle$ e-spin state, leaving behind excess population in the $|\downarrow\rangle$ state. The generated polarization persists after trion recombination if the spin precession period is less than the recombination time [26–28], which is the case in our experiment.

The weaker oscillations observed for negative delays are due to mode locking of spins [2]. If the individual e-spin coherence time T_2 is longer than the pulse repetition period T_R, there is constructive interference for spins that satisfy the phase synchronization condition (PSC) $\omega = 2\pi N/T_R$, where N is an integer and ω is the spin precession frequency. The negative delay signal is fairly weak for low pump intensities, as in Fig. 2(a), and stronger at higher pump intensities, as in Fig. 2(b). By measuring mode locking for several different values of T_R, we estimate T_2 at 100–200 ns for this sample, an order of magnitude smaller than the T_2 measured in Ref. [2]. We assign this difference to the smaller volume of our QDs [9,16,23] compared to those of Ref. [2].

Surprisingly, the TRFR signal is comparable to the TRFE signal at the higher pump intensity [Fig. 2(b)], even though the TRFR is expected to be near zero for $\delta_{\mathrm{probe}} = 0$. At this intensity, nearly all optically active electrons are excited to the trion state by a single pulse (roughly a π pulse). This result is the first hint of physics beyond simply pumping electrons into the $|\downarrow\rangle$ state through real transitions. As illustrated in Fig. 2(c), nonsynchronized e spins can be rotated into the x direction for $\delta_{\mathrm{QD}} \neq 0$. The first pulse generates a spin polarization along $-\hat{z}$, which then precesses about the magnetic field. If the spin is not synchronized to the pulse train, there is an S_y component just before the next pulse in the train. Since fast $\sigma^{\pm}$ pulses cause spin rotation about z [7,29–34], these spins will acquire a component along x. Thus, the pulses play the dual role of polarizing spins along z and rotating them about z. This optical spin rotation can be described either by the optical Stark effect [7,29,33] or by geometric phases [31,34]. In both descriptions a short pulse drives electrons in only one of the spin states shown in Fig. 1(c) up to the trion and back down within the pulse length. This produces a relative phase shift between the spin states, i.e., a spin rotation about z. The angle of rotation is a decreasing

function of the detuning, and the direction of rotation depends on the sign of detuning.

The nuclear dynamics are significantly changed by a nonzero S_x since the nuclear spin-flip rates $w_\pm$ are proportional to $(1 \pm 2S_x)$ [35]. When $S_x \neq 0$ the nuclear spin-flip rate from spin up to down, w_-, is different from the rate to flip from down to up, w_+ [36]. An intuitive description of the electron and nuclear spin dynamics that result can be given based on Figs. 2(d) and 2(e). Consider a negatively detuned QD with a precession frequency close to a PSC. If ω is a bit smaller (larger) than the PSC, S_x will be positive (negative) and make nuclear spins more likely to flip up (down) [37]. In both cases, the nuclear polarization will change to move ω toward the PSC [Fig. 2(e), right]. For a positively detuned QD, the sign of S_x is opposite, so the nuclear polarization changes to move ω away from the PSC [Fig. 2(e), left]. The positively detuned QDs settle at "antisynchronized" frequencies, which results in a much lower spin polarization.

A manifestation of these nuclear dynamics is observed in Figs. 3(a) and 3(b), which plot the measured amplitude of Faraday rotation and ellipticity, respectively, versus δ_{probe} for a series of pump intensities. The rotation and ellipticity are very nearly the expected odd and even functions of δ_{probe} at the lowest pump intensity, 60 W/cm^2, indicating the distribution of spin-polarized QDs is symmetric and spectrally narrow. With increasing pump intensity, the spectral features in Figs. 3(a) and 3(b) are broader and clearly shift toward lower probe energies. Because of this spectral shift, the Faraday rotation signal at zero detuning is quite large at high intensity, as observed in Fig. 2(b). The broadening can be explained by higher pump intensities polarizing wider spectral distributions of QDs. The spectral shifts of ~0.4 meV for the ellipticity and ~0.7 meV for the rotation at the highest pump intensity are due to a higher density of synchronized e spins for negative δ_{QD} and a lower density of synchronized e spins for positive δ_{QD}.

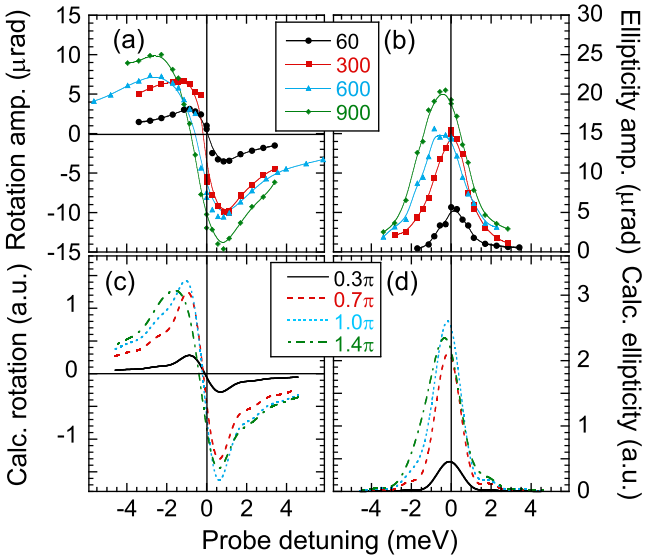

FIG. 3 (color online). (a,b) Positive delay amplitude of the experimental (a) TRFR and (b) TRFE as a function of probe detuning from the pump for a series of pump intensities (in W/cm^2). Lines are provided to guide the eye. (c,d) Theoretical calculation of the positive delay amplitude of (c) rotation and (d) ellipticity for a series of pulse areas (shown in the inset).

We qualitatively reproduce these spectral shifts in Figs. 3(c) and 3(d) by simulating the e-spin interaction with the pulse train and the feedback effect of the nuclei on the e-spin precession frequency. We first find steady-state expressions for the spin components as a function of the precession frequency ω, the Rabi frequency Ω, and the detuning δ_{QD}. Analytical expressions are obtained for the response of an arbitrary e-spin state to a single pulse, and then the solution for a pulse train is determined. Figure 4(a) displays the calculated steady-state e-spin vector components right after a pulse as functions of the spin precession frequency. The troughs in S_z correspond to frequencies meeting the PSC.

The nuclear spin-flip rates depend on the rate at which optical transitions occur and on the energy mismatch between nuclear and e-spin splittings [19], with asymmetry in the nuclear spin-flip directions determined by S_x:

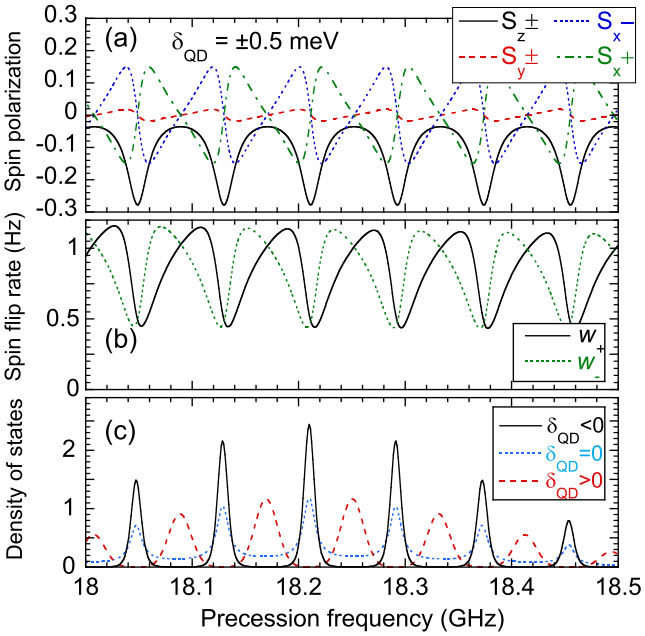

FIG. 4 (color online). (a) Calculated components of the e-spin polarization (labeled by direction and by the sign of detuning) just after a pulse as a function of the spin precession frequency, for QDs detuned $\delta_{\text{QD}} = \pm 0.5$ meV from pump pulses of area π. Complete spin polarization corresponds to $|\boldsymbol{S}| = 0.5$. (b) Calculated nuclear spin-flip rates as a function of e-spin precession frequency for $\delta_{\text{QD}} = -0.5$ meV and π pulses. (c) Calculated steady-state density of states as a function of e-spin precession frequency for $\delta_{\text{QD}} = -0.8$, 0, $+0.8$ meV and π pulses.

$$w_{\pm} \propto \frac{W(\Omega, \delta_{\mathrm{QD}})}{2T_R} \frac{[1 + 2S_z]}{\omega^2}[1 \pm 2S_x], \qquad (1)$$

where W is the transition probability of the allowed electron to trion transition. The rates are plotted in Fig. 4(b) as functions of the precession frequency. Using Eq. (1), we solve numerically for the steady-state nuclear polarization probability distribution. From the steady-state nuclear polarization distribution we find the density of states (DOS) of the electronic precession frequencies for a series of detunings for each pump pulse area. Figure 4(c) shows the results of our calculations; the dramatic effect of the detuning is seen by comparing the DOS of the positive with that of the negative detuning. For negative δ_{QD} the DOS is concentrated at the PSCs, giving good mode locking; i.e., the net S_z component averaged over all the QDs is large. For positive δ_{QD} the DOS is concentrated in between the PSCs, giving poor mode locking. This asymmetry gives rise to the spectral shift in the calculated rotation and ellipticity spectra in Figs. 3(c) and 3(d), the magnitude of which is determined by the contrast in the degree of synchronization between negative and positive δ_{QD}. Interestingly, the direction of this shift should not change with reversed magnetic field direction or with opposite pulse helicity (experimentally confirmed). Only the sign of the g factor determines the direction of the shift.

These results have important implications not only for using e spins as qubits but also for controlling the nuclear spins, narrowing their distribution, and perhaps making possible their use for the storage of quantum information [38]. Although we have not demonstrated a significant net nuclear polarization in the present study, we have shown that the nuclear dynamics can be controlled and the resulting distributions are more stable for detuned pulses than for resonant pulses. A good indication of the improved stability is the nearly zero density of states in Fig. 4(c) between stable frequencies for detuned QDs. We expect that one could significantly polarize nuclei using this technique by slowly changing the magnetic field while the pulse train locks QDs to their initial precession frequency. The nuclear polarization must slowly increase to make up for the decreasing magnetic field. In conclusion, we have shown that by using optically detuned pulses we can control the effects of the hyperfine interaction of the electron with the nuclear spin. This Letter provides an additional handle toward optical control of the nuclear QD spins.

This work is supported by the U.S. Office of Naval Research. S. E. E. received additional support from the NRC/NRL.

[1] J. R. Petta *et al.*, Science **309**, 2180 (2005).
[2] A. Greilich *et al.*, Science **313**, 341 (2006).
[3] E. A. Stinaff *et al.*, Science **311**, 636 (2006).
[4] M. Atature *et al.*, Science **312**, 551 (2006).
[5] X. Xu *et al.*, Phys. Rev. Lett. **99**, 097401 (2007).
[6] A. Greilich *et al.*, Phys. Rev. Lett. **96**, 227401 (2006).
[7] J. Berezovsky *et al.*, Science **320**, 349 (2008).
[8] I. A. Merkulov, A. L. Efros, and M. Rosen, Phys. Rev. B **65**, 205309 (2002).
[9] A. V. Khaetskii, D. Loss, and L. Glazman, Phys. Rev. Lett. **88**, 186802 (2002).
[10] W. A. Coish and D. Loss, Phys. Rev. B **70**, 195340 (2004).
[11] A. S. Bracker *et al.*, Phys. Rev. Lett. **94**, 047402 (2005).
[12] P.-F. Braun *et al.*, Phys. Rev. B **74**, 245306 (2006).
[13] D. Stepanenko *et al.*, Phys. Rev. Lett. **96**, 136401 (2006).
[14] C. Deng and X. Hu, Phys. Rev. B **73**, 241303(R) (2006).
[15] W. M. Witzel and S. Das Sarma, Phys. Rev. B **74**, 035322 (2006).
[16] W. Yao, R.-B. Liu, and L. J. Sham, Phys. Rev. B **74**, 195301 (2006).
[17] V. L. Korenev, Phys. Rev. Lett. **99**, 256405 (2007).
[18] P. Maletinsky *et al.*, Phys. Rev. B **75**, 035409 (2007).
[19] A. Greilich *et al.*, Science **317**, 1896 (2007).
[20] M. N. Makhonin *et al.*, Appl. Phys. Lett. **93**, 073113 (2008).
[21] D. J. Reilly *et al.*, Science **321**, 817 (2008).
[22] J. Danon and Y. V. Nazarov, Phys. Rev. Lett. **100**, 056603 (2008).
[23] Ł. Cywiński, W. M. Witzel, and S. Das Sarma, Phys. Rev. Lett. **102**, 057601 (2009).
[24] Z. R. Wasilewski, S. Fafard, and J. P. McCaffrey, J. Cryst. Growth **201–202**, 1131 (1999).
[25] J. D. Jackson, *Classical Electrodynamics* (Wiley, New York, 1999), 3rd ed., Chap. 7.
[26] A. Shabaev *et al.*, Phys. Rev. B **68**, 201305(R) (2003).
[27] S. E. Economou *et al.*, Phys. Rev. B **71**, 195327 (2005).
[28] M. V. G. Dutt *et al.*, Phys. Rev. Lett. **94**, 227403 (2005).
[29] M. Combescot and O. Betbeder-Matibet, Solid State Commun. **132**, 129 (2004).
[30] C. E. Pryor and M. E. Flatte, Appl. Phys. Lett. **88**, 233 108 (2006).
[31] S. E. Economou *et al.*, Phys. Rev. B **74**, 205415 (2006).
[32] S. G. Carter, Z. Chen, and S. T. Cundiff, Phys. Rev. B **76**, 201308(R) (2007).
[33] D. Press *et al.*, Nature (London) **456**, 218 (2008).
[34] A. Greilich *et al.*, Nature Phys. 5, 262 (2009).
[35] M. I. Dyakonov and V. I. Perel, Zh. Eksp. Teor. Fiz. **65**, 362 (1973) [Sov. Phys. JETP **38**, 177 (1974)].
[36] We treat each nucleus as a spin-1/2 system. This provides considerable simplification but still captures the main physics.
[37] We assume clockwise spin precession about the magnetic field, which gives results consistent with the experiment.
[38] J. M. Taylor, C. M. Marcus, and M. D. Lukin, Phys. Rev. Lett. **90**, 206803 (2003).